Spin Pumping at the Magnetic Insulator (YIG)/Normal Metal (Au) Interfaces

B. Heinrich,[1,*] C. Burrowes,[1] E. Montoya,[1] B. Kardasz,[1] E. Girt,[1] Young-Yeal Song,[2] Yiyan Sun,[2] and Mingzhong Wu[2]

[1]*Physics Department, Simon Fraser University, 8888 University Drive, Burnaby, British Columbia, V5A 1S6, Canada*

[2]*Physics Department, Colorado State University, Fort Collins, Colorado 80523, USA*

(Received 19 April 2011; published 2 August 2011)

Spin injection across the ferrimagnetic insulator (YIG)/normal metal (Au) interface was studied by ferromagnetic resonance. The spin mixing conductance was determined by comparing the Gilbert damping in bare YIG films with those covered by a Au/Fe/Au structure. The Fe layer in Au/Fe/Au acted as a spin sink as displayed by an increased Gilbert damping parameter α compared to that in the bare YIG. In particular, for the 9.0 nm YIG/2.0 nm Au/4.3 nm Fe/6.1 nm Au structure, the YIG and Fe films were coupled by an interlayer exchange coupling, and the exchange coupled YIG exhibited an increased Gilbert damping compared to the bare YIG. This relationship between static and dynamic coupling provides direct evidence for spin pumping. The transfer of spin momentum across the YIG interface is surprisingly efficient with the spin mixing conductance $g_{\uparrow\downarrow} \simeq 1.2 \times 10^{14}$ cm^{-2}.

DOI: 10.1103/PhysRevLett.107.066604 PACS numbers: 72.25.−b, 72.15.Lh, 75.70.−i, 76.50.+g

Giant magnetoresistance and spin transfer torque devices [1] are based on spin-polarized electron currents. In these devices, the spin and electron transport are not separated and therefore are affected by typical limitations of electronic circuits: circuit capacitance, heat generation, and electron migration. Recently, attention has turned to developing ideas and systems where spin transfer torque can be achieved by pure spin currents. A newly emerging field called spin caloritronics [2] addresses the generation of a spin current by a thermal gradient. In his pioneering work, Slonczewski has shown that a higher efficiency in spin transfer torque devices can be achieved by using spin transport driven by thermal gradients in magnetic insulator/normal metal structures [3]. Magnetic insulators, yttrium iron garnets (YIG), in particular, have very low magnetic losses, and by heat gradient one can create a large number of low loss magnons, allowing one to generate an appreciable pure spin current.

In order to pursue this approach, one has to establish the effectiveness of spin momentum transfer across a magnetic insulator (MI)/normal metal (NM) layer interface. Xiao *et al.* faced a similar situation in the theoretical treatment of the spin Seebeck effect [2]. They have shown that the transfer of spin momentum is governed by the real part of interface spin mixing conductance, $g_{\uparrow\downarrow}$, which at the ferromagnetic (FM)/NM interface [4] is given by

$$g_{\uparrow\downarrow} = \frac{1}{2}\sum_m (|r_{\uparrow,m} - r_{\downarrow,m}|^2 + |t_{\uparrow,m} - t_{\downarrow,m}|^2), \qquad (1)$$

where $r_{\uparrow(\downarrow),m}$ and $t_{\uparrow(\downarrow),m}$ are the spin majority (minority) reflectivity and transmission parameters, respectively, of a NM electron in the channel m impinging on the FM/NM interface. The spin mixing conductance is experimentally well established in metallic systems and is found to be in agreement with theoretical predictions [5,6]. However, there is an important difference between the metallic FM/NM and MI/NM interfaces. In the metallic interface, $g_{\uparrow\downarrow}$ is governed by the sum $\sum_m (|r_{\uparrow(\downarrow),m}|^2 + |t_{\uparrow(\downarrow),m}|^2)$. Since this expression adds 1 to each channel m, for the metallic interface one has $g_{\uparrow\downarrow} \approx 0.75n^{2/3}$, where n is the density of electrons per spin in the NM layer [5]. The situation at the MI/NM interface is different. The transmission parameters are zero, and the absolute values of the reflectivity parameters are one. Bauer pointed out that $g_{\uparrow\downarrow}$ even in this case is not zero [7]. The reason is that the reflectivity parameter includes the phase, $r_{\uparrow(\downarrow)} = 1e^{i\varphi_{\uparrow(\downarrow),m}}$, that is dependent on the channel number m resulting in a nonzero value for $g_{\uparrow\downarrow}$:

$$g_{\uparrow\downarrow} = \sum_m [1 - \cos(\varphi_{\uparrow,m} - \varphi_{\downarrow,m})]. \qquad (2)$$

For a small difference $\varphi_{\uparrow,m} - \varphi_{\downarrow,m}$, the spin mixing conductance is proportional to the sum of $(\varphi_{\uparrow,m} - \varphi_{\downarrow,m})^2$. This is very different from metallic interfaces, where $g_{\uparrow\downarrow}$ is given by the number of impinging electrons. In metallic interfaces, these phase differences enter the imaginary part of $g_{\uparrow\downarrow}$ determining the interface gyromagnetic ratio (g factor). The imaginary part is known to be small compared to the real part of $g_{\uparrow\downarrow}$ [8] that enters the interface Gilbert damping. It is therefore of utmost importance to determine the contribution of these phase differences to the real part of $g_{\uparrow\downarrow}$ at the MI/NM interface.

Recently, Sandweg *et al.* [9] carried out studies of spin pumping efficiency across the YIG/Pt interface by using the inverse spin-Hall effect. In these studies, the dc voltage was measured across the Pt layer for different rf excitation modes. No quantitative interpretation of the data was presented. The main goal of this paper was to identify quantitatively the spin mixing conductance at the YIG/Au interface.

Spin pumping and interface damping.—The pumped magnetic current across the FM1/NM interface is given (see [4,5]) in a system with electron diffuse interface scattering by

$$\boldsymbol{I}_{\mathrm{sp}} = -\frac{g\mu_B}{4\pi}\mathrm{Re}(2g_{\uparrow\downarrow})\left[\boldsymbol{u}\times\frac{\partial \boldsymbol{u}}{\partial t}\right], \tag{3}$$

where $\boldsymbol{u}$ is the unit vector in the instantaneous direction of the magnetic moment, g is the Landé factor in FM1, and μ_B is the Bohr magneton. For small precessional angles of the magnetic moment in FM1, the pumped magnetic moment is almost entirely transverse to the static magnetic moment, and the FM2 layer in FM1/NM/FM2 will act as a perfect sink [10]. In YIG/Au/Fe/Au magnetic double layer structures, the ferromagnetic resonance (FMR) fields corresponding to the YIG and Fe films are separated by several kOe; therefore, the YIG and Fe films are not involved at the same time in interchanging spin currents. When the Au films covering YIG are much thinner than the spin diffusion length in Au (35 nm [6]), one can in a very good approximation neglect the loss of accumulated spin momentum in the Au layer. The spin current generated at the YIG/Au interface leads to an increased Gilbert damping in YIG and in this approximation is given by

$$\alpha_{\mathrm{sp}} = \frac{g\mu_B}{4\pi M_s} g_{\uparrow\downarrow}\frac{1}{d}, \tag{4}$$

where $4\pi M_s$ is the saturation induction and d is the thickness of the YIG film.

Sample preparation and FMR measurements.—YIG $[Y_3Fe_2(FeO_4)_3]$ films with thicknesses of 5 and 9 nm grown on (111) $Gd_3Ga_5O_{12}$ substrates were prepared by pulsed laser deposition. The deposition was performed in high purity oxygen for 9 min with the substrate at 790 °C and the oxygen pressure held at 0.1 torr. Right after the deposition, the YIG films were annealed at the same temperature and oxygen pressure for 10 min. The thickness of the YIG films was determined by low angle x-ray diffraction. The YIG films were characterized by x-ray photoelectron spectroscopy. The Au and Fe films were deposited by molecular beam epitaxy at pressures in the low 10^{-10} torr at room temperature.

In the presented studies, the sample S1 is 9 YIG/2 Au/4.3 Fe/6.1 Au and S2 is 9 YIG/6.1 Au/4.3 Fe/6.1 Au, with the numbers indicating film thickness in nanometers. The x-ray photoelectron spectroscopy spectra indicated Fe was deficient at the YIG surface. The atomic ratio Fe/Y for both samples was 0.55, while, according to the chemical formula, it is expected to be 1.7. The atomic ratio O/Y was found to be 4 and 6 for S1 and S2, respectively. The expected ratio by the chemical formula is 4. This indicates that the oxygen concentration in S2 was higher than that in S1. The difference in chemical composition at the YIG surface compared to its bulk is caused by the surface chemistry during pulsed laser deposition, and it is similar to thick YIG films. Cleaning of the YIG surface by a hydrogen atom gun led to splitting and broadening of the FMR lines and therefore was not used. The Au and Fe films were polycrystalline.

FMR measurements were carried out at 10, 14, 24, and 36 GHz by using an Anritsu microwave generator with a static magnetic field along the film surface. Samples inserted in microwave cavity were 3×4 mm^2. The microwave power was adjusted for a small precessional angle. Bare YIG films, by eye inspection, exhibited only one resonance peak corresponding to a homogeneous distribution of the rf magnetization across the YIG film, the $k=0$ magnon mode. However, in order to fit these apparently single FMR peaks, one needs to take the superposition of up to three closely separated Lorentzian lines; see Fig. 1. This indicates that the films consisted of up to three regions having slightly different saturation magnetizations. The intrinsic FMR linewidth ΔH (half width at half maximum) in the YIG films was linearly dependent on the microwave angular frequency $\omega(=2\pi f)$ but exhibited an appreciable zero frequency offset; see Fig. 2. The linear slope is consistent with Gilbert damping:

$$\Delta H = \alpha\frac{\omega}{\gamma}, \tag{5}$$

where γ is the absolute value of the gyromagnetic ratio and α is the Gilbert damping parameter. The zero frequency offset is caused by long range magnetic inhomogeneities.

In the bare YIG films, the Gilbert damping parameter was small: $\alpha \simeq 0.0006$. The zero frequency offset did not

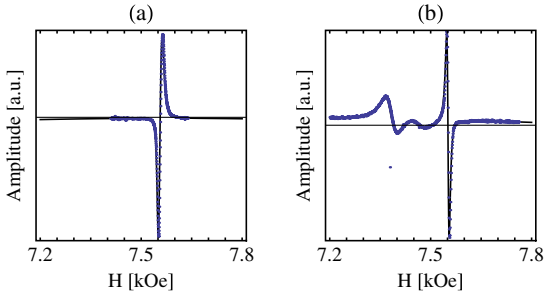

FIG. 1 (color online). The field derivative of the FMR signal as a function of the external field. (a) $f = 23.988$ GHz, bare YIG 9.0 nm. The FMR line required 3 Lorentzian absorption lines with the following parameters: $H_{\mathrm{res},1} = 7.556$ kOe, $\Delta H_1 = 9.7$ Oe, and $\mathrm{RA}_1 = 60\%$; $H_{\mathrm{res},2} = 7.551$ kOe, $\Delta H_2 = 7.7$ Oe, and $\mathrm{RA}_2 = 31\%$; and $H_{\mathrm{res},2} = 7.563$ kOe, $\Delta H_2 = 7.2$ Oe, and $\mathrm{RA}_3 = 9\%$. (b) $f = 23.9751$ GHz, YIG/2.0 Au/4.3 Fe/6.1 Au. The three peaks in the bare sample became well split due to ferromagnetic coupling between the YIG and Fe layers. $H_{\mathrm{res},1} = 7.380$ kOe, $\Delta H_1 = 31.3$ Oe, and $\mathrm{RA}_1 = 49\%$; $H_{\mathrm{res},2} = 7.468$ kOe, $\Delta H_2 = 50.6$ Oe, and $\mathrm{RA}_1 = 40\%$; and $H_{\mathrm{res},3} = 7.552$ kOe, $\Delta H_3 = 6.3$ Oe, and $\mathrm{RA}_3 = 11\%$. RA represents the relative area of the sample with the corresponding FMR parameters. Notice that the FMR lines for the areas (1) and (2) are shifted towards lower magnetic fields and the line (3) is unshifted from the FMR field of the bare YIG film. The areas (1) and (2) are coupled by ferromagnetic interlayer exchange coupling to the Fe layer.

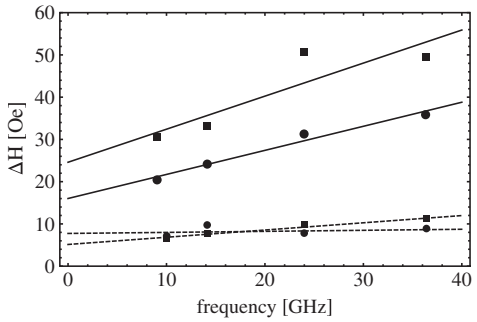

FIG. 2. FMR linewidth $\Delta H(f)$ as a function of microwave frequency for sample S1: 9.0 YIG/2.0 Au/4.3 Fe/6.1 Au and the bare corresponding YIG film. The solid square and circle points correspond to the areas (2) and (1) in Fig. 1 which are coupled by ferromagnetic exchange coupling to the Fe layer. The solid lines correspond to S1. The dashed lines correspond to the bare YIG sample. The sample area (3) was not exchange coupled to the Fe film and showed no change in $\Delta H(f)$ compared to that in the bare YIG. The increase in zero frequency offset in $\Delta H_{1,2}(f = 0)$ for the exchange-coupled areas compared to the bare YIG is caused by an inhomogeneous distribution of the interlayer exchange coupling.

disappear in the perpendicular FMR (the field perpendicular to the film surface) and therefore was not caused by two-magnon scattering indicating that the films were accompanied by long range magnetic inhomogeneities [11]; see Fig. 2. The FMR line position and $\Delta H(f)$ did not change by depositing a thin Au film over YIG.

Results and discussion.—The saturation induction was determined by SQUID magnetometry, and it was found to be 1.31 kG. The lower value compared to the bulk was perhaps caused by a deficiency of the Fe atomic concentration at the interfaces. The effective perpendicular demagnetizing field $4\pi M_{\text{eff}} = 4\pi M_s - H_{u,\perp}$ ($H_{u,\perp}$ is the uniaxial perpendicular anisotropy field) and the g factor in the YIG films were determined from the FMR data at different microwave frequencies; see Table I. For the 4.3 Fe film, $4\pi M_{\text{eff}} = 10.6$ kOe. Spin pumping was measured in samples S1 and S2. The Gilbert damping contribution to the FMR linewidth in YIG had two contributions: (a) the bulk contribution α_b as measured in bare YIG films and (b) the interface spin pumping contribution is in the ballistic limit given by Eq. (4).

Important results, shown in Figs. 1 and 2, were obtained on S1. Deposition of 2.0 Au/4.3 Fe/6.1 Au on YIG resulted in a well-defined splitting of the original three closely spaced FMR peaks; see Fig. 1. This means that the 2.0 nm Au spacer resulted in an interlayer exchange coupling J_{ex} between the YIG and Fe layers. In fact, the three peaks represent three different samples. The peak at the highest field remained very near the FMR field for the bare YIG, but the other two peaks became visibly downshifted by 70 and 138 Oe due to magnetic coupling. The surface roughness of the YIG films measured by an atomic force microscope is 0.5 nm, which results in negligible magnetostatic coupling between the YIG and Fe film of 1×10^{-4} erg/cm^2. Therefore the layers are coupled by ferromagnetic interlayer exchange coupling $J_{\text{ex}} = +(0.08 \text{ and } 0.15)$ erg/cm^2 for the area (1) and (2), respectively. Even more importantly, the slope of the FMR linewidth as a function of microwave frequency, $\Delta H(f)$, increased for the coupled areas, while the uncoupled area showed no increase in this slope. The absence of exchange coupling in the highest FMR peak indicates that the electrons in the Au layer did not experience the spin-dependent potential at the YIG/Au interface. This also means that one cannot expect any contribution to spin pumping as the spin mixing conductance requires a spin-dependent interface potential; see Eq. (2). However, the areas exhibiting exchange coupling experienced the spin-dependent potential and resulted in spin pumping [12].

In fact, Figs. 1 and 2 represent the first clear experimental demonstration of this relationship between the static interlayer exchange coupling and the spin pumping mechanism.

The RKKY-induced spin density in the NM oscillates with the Fermi spanning k wave vectors [13] and decreases with the thickness of the NM spacer layer. This picture remains valid for polycrystalline layers, where the overall coupling strength and oscillatory period are averaged over the orientation of crystalline grains. Because of interface roughness, this coupling quickly approaches zero and is usually zero for the Au spacer thickness above 3 nm [14]. The spin pumping contribution creates an accumulated spin density at the YIG/Au interface, and its transport across the Au spacer is governed by spin diffusion equations. The accumulated spin density decreases with an increasing distance from the YIG/Au interface due to the loss of spin momentum by a spin flip relaxation mechanism. The length scale of penetration of the accumulated spin density from the YIG/Au interface is given by the spin diffusion length, which in Au spacers was found to be of 35 nm; see [10]. For a Au thickness significantly less

TABLE I. Magnetic fitting parameters for samples S1: 9.0 YIG/2.0 Au/4.3 Fe/6.1 Au and S2: 9.0 YIG/6.1 Au/4.3 Fe/6.1 Au.

Magnetic properties	$g_{\uparrow\downarrow}$ [10^{14} cm^{-2}]	$4\pi M_{\text{eff}}$ [kOe]	g factor	α [10^{-3}]	J_{ex} [erg/cm^2]
S1 (upper solid line in Fig. 2)	1.2	1.885	2.027	2.21	0.15
S1 (lower solid line in Fig. 2)	1.1	1.885	2.027	1.62	0.08
S2 (squares in Fig. 3)	1.3	1.966	2.02	2.40	0
Bare YIG for S2 (circles in Fig. 3)	N/A	1.966	2.02	0.71	N/A

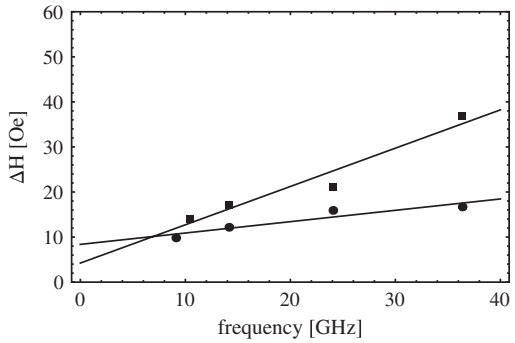

FIG. 3. FMR linewidth as a function of microwave frequency for sample S2: 9.0 YIG/6.1 Au/4.3 Fe/6.1 Au (squares) and the corresponding bare YIG film (circles). The FMR lines are described by two Lorentzian lines. Spin pumping contributions from both areas were similar. For clarity, the most intense line is shown.

than the spin diffusion length, this decrease is only minor and Eq. (4) is nearly correct.

The sample S2 does not show any appreciable shift in the FMR field compared to that in the bare YIG; therefore, the static interlayer exchange coupling for the thick 6.1 Au spacer averages to zero due to interface roughness. However, the slope of $\Delta H(f)$ clearly increased compared to that in the bare YIG; see Fig. 3. This is expected because the thickness of the Au layer is significantly smaller than the spin diffusion length.

In addition, spin pumping experiments were performed on a sample 5 YIG/6.1 Au/2.9 Fe/4.1 Au. In this case, FMR measurements were made on the bare YIG as well as following the growth of 4.3 Au. The 5 YIG/4.3 Au sample was then placed back into the molecular beam epitaxy system, where a small oxidation of Au was removed by sputtering under oblique incidence. The remaining structure was then deposited and followed by FMR measurements. The resulting $g_{\uparrow\downarrow 5\mathrm{YIG}} \simeq 1 \times 10^{14}$ cm^{-2} was found in agreement with the results carried out by using the 9 YIG films, proving that spin pumping is an interface effect. Spin pumping at the YIG/Au interface is a robust effect as it was unchanged by sputtering of the Au overlayer.

The increase in the Gilbert damping in samples S1 and S2 was interpreted by using a full spin pumping theory, which is based on magnetoelectronics equations; see Eq. (14) in Ref. [10]. The spin mixing conductances at the YIG/Au interfaces are large (see Table I), and they are an appreciable fraction of that found for the Fe/Au(001) interface: $g_{\uparrow\downarrow,\mathrm{Fe}} = 1.1 \times 10^{15}$ cm^{-2}.

Conclusions.—By using FMR measurement of Gilbert damping in thin YIG films and YIG/Au/Fe/Au structures, it was shown that the YIG/Au interface exhibits a strong spin pumping conductance which is ~11% of that observed in the metallic interface of Fe/Au. The strength of the spin mixing conductance was found somewhat inhomogeneous across the YIG surface. This inhomogeneity is not surprising considering that the thin YIG film surface chemistry deviates from that of the bulk. A large spin mixing conductance can provide an effective source of pure spin currents for spintronics circuits. YIG films over a micrometer in thickness exhibit very narrow FMR linewidths and can be then brought to a large angle of precession with a moderate microwave power. This can provide large dc spin currents. For an angle of precession in an extreme limit of $\pi/2$ (achievable in lateral nanostructures where magnon-magnon scattering can be suppressed by the selection rules), the dc magnetic moment current density can reach values of $1 \times 10^{24} \mu_B/\mathrm{cm}^2\,\mathrm{s}$ at 10 GHz. This shows that a large number of magnons can be generated by either microwave power or thermal gradients, allowing one to design spintronics devices based on these novel magnetic insulator/normal metal interfaces.

Financial support from the Natural Sciences and Engineering Research Council of Canada, the Canadian Institute for Advanced Research, the U.S. National Science Foundation, and the U.S. National Institute of Standards of Technology is gratefully acknowledged.

*Corresponding author.
bheinric@sfu.ca

[1] I. Zutic, J. Fabian, and S. Das Sarma, Rev. Mod. Phys. **76**, 323 (2004).
[2] J. Xiao, G. E. W. Bauer, K. C. Uchida, E. Saitoh, and S. Maekawa, Phys. Rev. B **81**, 214418 (2010).
[3] J. C. Slonczewski, Phys. Rev. B **82**, 054403 (2010).
[4] Y. Tserkovnyak, A. Brataas, and G. E. W. Bauer, Phys. Rev. Lett. **88**, 117601 (2002).
[5] B. Heinrich, Y. Tserkovnyak, G. Woltersdorf, A. Brataas, R. Urban, and G. E. W. Bauer, Phys. Rev. Lett. **90**, 187601 (2003).
[6] B. Kardasz, O. Mosendz, B. Heinrich, Z. Liu, and M. Freeman, J. Appl. Phys. **103**, 07C509 (2008).
[7] G. Bauer (private communication).
[8] Y. Tserkovnyak, A. Brataas, G. Bauer, and B. Halperin, Rev. Mod. Phys. **77**, 1375 (2005).
[9] C. Sandweg, Y. Kajiwara, K. Ando, E. Saitoh, and B. Hillebrands, Appl. Phys. Lett. **97**, 252504 (2010).
[10] B. Kardasz and B. Heinrich, Phys. Rev. B **81**, 094409 (2010).
[11] G. Woltersdorf and B. Heinrich, Phys. Rev. B **69**, 184417 (2004).
[12] E. Simanek and B. Heinrich, Phys. Rev. B **67**, 144418 (2003).
[13] P. Bruno, J. Phys. Condens. Matter **11**, 9403 (1999).
[14] Z. Celinski and B. Heinrich, J. Magn. Magn. Mater. **99**, L25 (1991).